Prosurvival kinase PIM2 is a therapeutic target for eradication of chronic myeloid leukemia stem cells

Leyuan Ma[a,1], Magnolia L. Pak[a,1], Jianhong Ou[a], Jun Yu[a], Pamela St. Louis[b], Yi Shan[c], Lloyd Hutchinson[d], Shaoguang Li[c], Michael A. Brehm[b], Lihua Julie Zhu[a,b,e], and Michael R. Green[a,2]

[a]Department of Molecular, Cell and Cancer Biology, University of Massachusetts Medical School, Worcester, MA 01605; [b]Program in Molecular Medicine, University of Massachusetts Medical School, Worcester, MA 01605; [c]Division of Hematology/Oncology, Department of Medicine, University of Massachusetts Medical School, Worcester, MA 01605; [d]Department of Pathology, University of Massachusetts Medical School, Worcester, MA 01605; and [e]Program in Bioinformatics and Integrative Biology, University of Massachusetts Medical School, Worcester, MA 01605

Contributed by Michael R. Green, April 5, 2019 (sent for review March 1, 2019; reviewed by Fang Liu and Kevin Struhl)

A major obstacle to curing chronic myeloid leukemia (CML) is the intrinsic resistance of CML stem cells (CMLSCs) to the drug imatinib mesylate (IM). Prosurvival genes that are preferentially expressed in CMLSCs compared with normal hematopoietic stem cells (HSCs) represent potential therapeutic targets for selectively eradicating CMLSCs. However, the discovery of such preferentially expressed genes has been hampered by the inability to completely separate CMLSCs from HSCs, which display a very similar set of surface markers. To overcome this challenge, and to minimize confounding effects of individual differences in gene expression profiles, we performed single-cell RNA-seq on CMLSCs and HSCs that were isolated from the same patient and distinguished based on the presence or absence of BCR-ABL. Among genes preferentially expressed in CMLSCs is *PIM2*, which encodes a prosurvival serine-threonine kinase that phosphorylates and inhibits the proapoptotic protein BAD. We show that IM resistance of CMLSCs is due, at least in part, to maintenance of BAD phosphorylation by PIM2. We find that in CMLSCs, *PIM2* expression is promoted by both a BCR-ABL–dependent (IM-sensitive) STAT5-mediated pathway and a BCR-ABL–independent (IM-resistant) STAT4-mediated pathway. Combined treatment with IM and a PIM inhibitor synergistically increases apoptosis of CMLSCs, suppresses colony formation, and significantly prolongs survival in a mouse CML model, with a negligible effect on HSCs. Our results reveal a therapeutically targetable mechanism of IM resistance in CMLSCs. The experimental approach that we describe can be generally applied to other malignancies that harbor oncogenic fusion proteins or other characteristic genetic markers.

BCR-ABL | CML stem cells | imatinib resistance | PIM2 | targeted therapy

The hematopoietic malignancy chronic myeloid leukemia (CML) is a disorder characterized by increased and unregulated proliferation of predominantly myeloid cells, resulting in their abnormal accumulation in the bone marrow and peripheral blood (1). Approximately 95% of individuals with CML harbor a chromosomal abnormality resulting from a reciprocal translocation between chromosomes 9 and 22 [t(9, 22)], which produces an oncogenic fusion protein known as BCR-ABL (2, 3). ABL is a tyrosine kinase that in normal cells plays a role in cellular differentiation and regulation of the cell cycle (4). However, the t(9, 22) translocation creates a constitutively active ABL tyrosine kinase, which transforms myeloid progenitor cells by aberrantly activating downstream prosurvival signaling pathways, such as RAS/RAF/MEK/ERK, phosphatidylinositol 3-kinase (PI3K)/AKT, and JAK/STAT (4, 5).

The standard therapy for CML is imatinib mesylate (IM), a selective tyrosine kinase inhibitor that binds near the ATP-binding site of ABL and stabilizes the kinase in an inactive form, thereby inhibiting phosphorylation of its downstream substrates (6). Unfortunately, IM is not a curative therapy for CML due, at least in part, to the persistence of a small population of stem cells, called CML stem cells (CMLSCs), that are resistant to IM treatment (7–9). CMLSCs are not dependent on BCR-ABL activity for their survival (10), implying that CMLSCs depend on other survival pathways to sustain viability in the presence of IM. The identification of prosurvival genes that are preferentially expressed in CMLSCs compared with normal hematopoietic stem cells (HSCs) may shed light on the basis by which CMLSCs are innately resistant to IM and may also reveal potential therapeutic targets for selectively eradicating CMLSCs. Here we report the identification of a prosurvival kinase that is preferentially expressed in CMLSCs and promotes IM resistance. Our results reveal a mechanism of IM resistance in CMLSCs that is therapeutically targetable.

Results

PIM2 Is Significantly Up-Regulated in CMLSCs Relative to HSCs. To distinguish CMLSCs and HSCs, which display a similar set of cell surface markers ($CD34^+CD38^-CD90^+CD45RA^-$) (11, 12), we first captured ~600 $CD34^+CD38^-CD90^+CD45RA^-$ cells (~200 from each of three CML patient samples) and then used single-cell nested quantitative RT-PCR (qRT-PCR) to detect the presence or absence of the BCR-ABL transcript (*SI Appendix*, *Supplementary Materials and Methods* and Fig. S1). Once

Significance

Chronic myeloid leukemia (CML) is a hematopoietic cancer caused by the oncogenic fusion protein BCR-ABL. The first-line treatment for CML is the BCR-ABL inhibitor imatinib mesylate (IM). Like several other cancers, CML is propagated by a small population of stem cells, whose eradication is required to cure the disease. Unfortunately, CML stem cells (CMLSCs) are resistant to IM treatment. Here we show that PIM2, a serine/threonine kinase, is required for IM resistance in CMLSCs. Combined treatment with IM and a PIM inhibitor synergistically kills CMLSCs in culture and significantly prolongs survival in a mouse CML model, with a negligible effect on normal hematopoietic stem cells. Our results reveal a mechanism of IM resistance in CMLSCs that can be therapeutically targeted.

Author contributions: L.M., M.L.P., S.L., M.A.B., and M.R.G. designed research; L.M., M.L.P., P.S.L., and Y.S. performed research; L.H. contributed new reagents/analytic tools; L.M., M.L.P., J.O., J.Y., L.J.Z., and M.R.G. analyzed data; P.S.L. and M.A.B. assisted with experiments using the PDX mouse model; Y.S. and S.L. assisted with experiments using the CML mouse model; L.H. provided CML patient samples; and L.M., M.L.P., and M.R.G. wrote the paper.

Reviewers: F.L., Rutgers University; and K.S., Harvard Medical School.

The authors declare no conflict of interest.

Data deposition: The RNA-seq data have been deposited in the Gene Expression Omnibus (GEO) database, https://www.ncbi.nlm.nih.gov/geo (accession no. GSE81730).

[1]L.M. and M.L.P. contributed equally to this work.

[2]To whom correspondence should be addressed. Email: Michael.Green@umassmed.edu.

This article contains supporting information online at www.pnas.org/lookup/suppl/doi:10.1073/pnas.1903550116/-/DCSupplemental.

Published online May 8, 2019.

CMLSCs and HSCs were identified, we carried out single-cell RNA-seq on ∼48 CMLSCs and ∼48 HSCs from each patient (13).

Typically, we obtained ∼2.5 million mapped reads (>70% average mapping efficiency) and detected ∼5,000 genes (transcripts per million [TPM] >1) per cell (*SI Appendix*, Fig. S2 *A–D*). To ensure the quality of the analysis, we excluded cells with low-sequencing depth (<0.5 million mapped reads) and low coverage (<2,000 genes). Previous single-cell RNA-seq studies have found that the average gene expression of as few as 30 single cells highly correlates with that of the population control typically derived from >10,000 cells (14). Because our analysis involved a pure BCR-ABL$^+$ or BCR-ABL$^-$ population that consisted of a relatively small number of cells, we asked whether our small sample size was sufficient to mimic a larger population control. Consistent with the previous studies, we found that random sampling with increasing number of cells achieved a high correlation at ∼30 cells (*SI Appendix*, Fig. S2*E*), confirming the validity of using ∼48 cells to represent each population group.

The RNA-seq analysis revealed substantial differences in HSC and CMLSC gene expression patterns among the three patients with CML (*SI Appendix*, Fig. S3*A*), underscoring the contribution of individual variation. Furthermore, the correlation of overall gene expression among single cells from the same patient ranged from 0.27 to 0.61, with a median of 0.43, indicative of significant heterogeneity (*SI Appendix*, Fig. S3 *B–D*). Despite the heterogeneity of the gene expression pattern, we were able to identify genes that were significantly more highly expressed in CMLSCs than in HSCs (*SI Appendix*, Fig. S4 *A* and *B* and Dataset S1). Approximately 28% of these differentially expressed genes had modest total expression levels (10< TPM ≤100) (*SI Appendix*, Fig. S4 *C* and *D*). Gene set enrichment analysis (GSEA) revealed significant enrichment of Wnt and cadherin signaling pathways (*SI Appendix*, Fig. S4*E*), both of which have been shown to be required for maintaining CMLSC viability and drug resistance (15).

One of the most highly and significantly up-regulated genes in CMLSCs was *PIM2* (Fig. 1*A*). Intrapatient comparison confirmed that *PIM2* was more highly expressed in CMLSCs compared with HSCs in all three patients with CML (Fig. 1*B*). We also found that in mice, *Pim2* was expressed at a higher level in BCR-ABL$^+$ CML Lin$^-$Sca1$^+$Kit$^+$ (LSK) cells and long-term HSCs compared with in their normal BCR-ABL$^-$ counterparts (*SI Appendix*, Fig. S5).

PIM2 Promotes IM Resistance by Maintaining BAD Phosphorylation. PIM2 is a member of a family of serine/threonine protein kinases known to have oncogenic potential in several malignancies (16). PIM kinases promote cell survival by phosphorylating the proapoptotic BH3-only protein BAD at S112 (17), which prevents BAD from interacting with and inhibiting antiapoptotic BCL-2 family proteins (18). The availability of small-molecule PIM inhibitors (19) and the finding that *Pim*$^{-/-}$ mice are viable and fertile (20) make PIM2 an attractive therapeutic target.

Previous studies have shown that IM treatment of IM-sensitive CML cells leads to reduced phosphorylation of BAD, which is responsible, at least in part, for cell death (21). The IM resistance of CMLSCs raised the question of whether BAD phosphorylation is maintained following IM treatment. To address this issue, we FACS-sorted IM-resistant CMLSCs and, as a control, IM-sensitive CML progenitors from patient samples and performed intracellular staining for phosphorylated BAD (pBAD). As an additional control, we also analyzed IM-sensitive human CML K562 cells (22). We found that IM treatment of IM-sensitive CML progenitors and K562 cells resulted in a substantial decrease in pBAD levels (Fig. 1*C*), as expected, whereas IM treatment of CMLSCs did not substantially affect pBAD levels (Fig. 1*C* and *SI Appendix*, Fig. S6*A*). Notably, however, treatment with the small-molecule pan-PIM inhibitor AZD1208 (19) substantially reduced pBAD levels in CMLSCs,

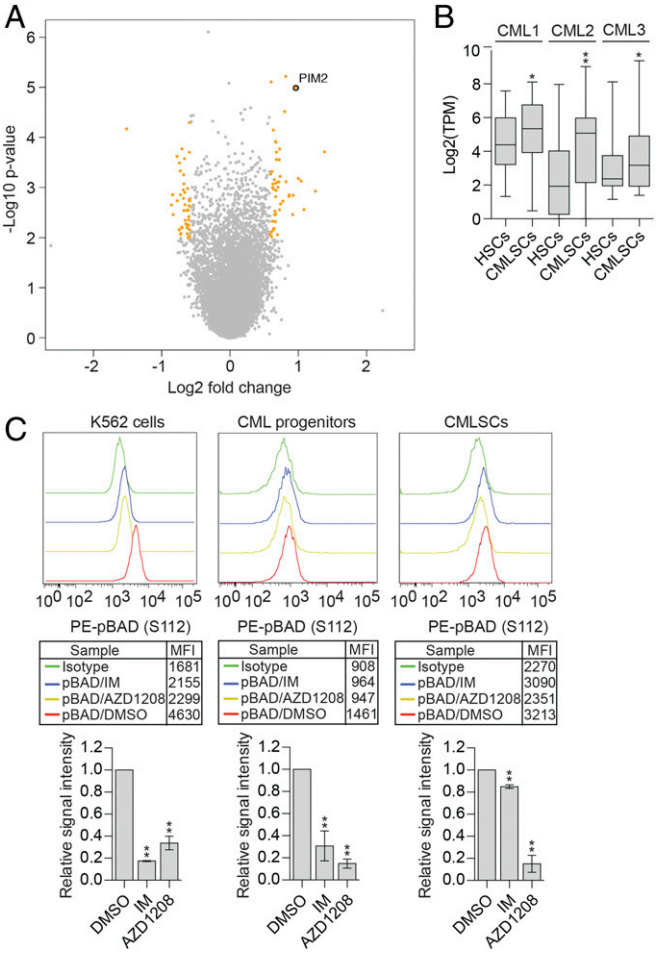

Fig. 1. PIM2 is significantly up-regulated in CMLSCs relative to HSCs and promotes IM resistance by maintaining BAD phosphorylation. (*A*) Volcano plot showing the significance (*y*-axis, −log10 *P* value) and differential expression (*x*-axis, log2 fold change) for genes identified by the RNA-seq analysis. Genes with $P < 0.01$ and fold change >1.5 or <1/1.5 are highlighted in orange, and genes that are not significantly changed are indicated in gray. *PIM2* is shown. (*B*) Boxplot showing the log2(TPM) value of *PIM2* from intrapatient comparison in three CML samples. Boxed areas span the first to third quartiles, the center line represents the mean, and whiskers represent maximum or minimum observations. $n = ∼48$ biological replicates. (*C*) Phospho-flow analysis showing intracellular staining of pBAD (S112) levels in DMSO-, IM-, and AZD1208-treated K562 cells; CML progenitors (CD34$^+$CD38$^+$); and CMLSCs (CD34$^+$CD38$^-$CD90$^+$). IgG was used for control staining. (*Upper*) Representative FACS histograms. The geometric mean fluorescence intensity (MFI) values are indicated in the boxed region. (*Lower*) Quantification of $n = 3$ or 4 biological replicates. Error bars indicate SEM. $*P \le 0.05$; $**P \le 0.01$.

CML progenitors, and K562 cells (Fig. 1*C* and *SI Appendix*, Fig. S6 *A* and *B*). Collectively, these results indicate that IM resistance of CMLSCs is due, at least in part, to maintenance of BAD phosphorylation by PIM2.

***PIM2* Expression in CMLSCs Is Promoted by Both a BCR-ABL–Dependent STAT5-Mediated Pathway and a BCR-ABL–Independent STAT4-Mediated Pathway.** Previous studies have shown that *PIM2* expression is promoted by STAT5 (23), which we confirmed in IM-sensitive K562 cells (*SI Appendix*, Fig. S7 *A* and *B*). Because STAT5 can be activated by BCR-ABL (24–26), we hypothesized that IM treatment would result in reduced PIM2 levels. Consistent with this hypothesis, IM treatment of K562 cells and CML progenitors significantly reduced *PIM2* mRNA

(Fig. 2*A*) and PIM2 protein levels (*SI Appendix*, Fig. S7*C*). Similar results were obtained in IM-sensitive BCR-ABL–transformed mouse Ba/F3 cells (*SI Appendix*, Fig. S7 *D* and *E*).

In contrast, IM treatment of IM-resistant human CMLSCs and mouse CML LSK cells did not significantly reduce *PIM2* levels (Fig. 2*A* and *SI Appendix*, Fig. S7 *F*–*J*). We hypothesized that in IM-resistant CMLSCs, *PIM2* expression is promoted by STAT5 as well as a BCR-ABL–independent STAT pathway. Analysis of published expression profiling results revealed that expression of STAT1, STAT2, and STAT4 were significantly higher in CMLSCs than in CML progenitors (*SI Appendix*, Fig. S8*A*), and thus we sought to examine the role of these STAT proteins in regulating *PIM2* expression. We and others have shown that IM resistance in CMLSCs can occur through mechanisms similar to those in CML cells that contain wild-type BCR-ABL but have developed IM resistance (27–29). Therefore, to initially evaluate the role of STAT1, STAT2, and STAT4, we used the experimentally tractable wild-type BCR-ABL IM-resistant CML cell line KCL22 (30), for which, like IM-resistant CMLSCs, treatment with IM did not affect *PIM2* expression (*SI Appendix*, Fig. S8*B*).

Knockdown of STAT4 in KCL22 cells significantly and reproducibly reduced *PIM2* expression following IM treatment, whereas knockdown of STAT1 or STAT2 did not (Fig. 2*B* and *SI Appendix*, Fig. S8*C*). Therefore, we focused on the role of STAT4 in regulating *PIM2* expression. In untreated KCL22 cells, *PIM2* expression was not affected by knockdown of STAT4 (Fig. 2*B* and *SI Appendix*, Fig. S8*C*) or STAT5 (Fig. 2*C* and *SI Appendix*, Fig. S8*D*) alone, but it was significantly reduced by combined knockdown of STAT4 and STAT5 (Fig. 2*C* and *SI Appendix*, Fig. S8*D*). Consistent with these results, chromatin immunoprecipitation (ChIP) experiments revealed that in untreated KCL22 cells, both phosphorylated STAT5 (pSTAT5) and phosphorylated STAT4 (pSTAT4) were enriched on the *PIM2* promoter, whereas following IM treatment, pSTAT5 levels were greatly reduced, and pSTAT4 levels were greatly increased (Fig. 2*D*).

Finally, we validated the key results of the experiments performed in KCL22 cells in IM-resistant CMLSCs. Similar to the results in KCL22 cells, knockdown of STAT4 in CMLSCs significantly reduced *PIM2* expression in the presence of IM (Fig. 2*E* and *SI Appendix*, Fig. S8*E*). In untreated CMLSCs, *PIM2* expression was not affected by knockdown of STAT4 (Fig. 2*E*) or STAT5 (Fig. 2*F* and *SI Appendix*, Fig. S8*F*) alone, but was significantly reduced by combined knockdown of STAT4 and STAT5 (Fig. 2*F* and *SI Appendix*, Fig. S8*F*). Collectively, these results show that in IM-resistant CML cells and CMLSCs, *PIM2* is regulated by both STAT4 and STAT5, and that following IM treatment, *PIM2* levels are maintained by a BCR-ABL–independent STAT4-based mechanism.

Combined Treatment with IM and the PIM Inhibitor AZD1208 Synergistically Increases Apoptosis of CMLSCs and Suppresses Colony Formation. The forgoing results suggest that IM resistance in CMLSCs is due to up-regulation of *PIM2*. In support of this idea, shRNA-mediated knockdown of *PIM2* sensitized CMLSCs to IM treatment (Fig. 3*A* and *SI Appendix*, Fig. S9*A*) due, at least in part, to increased apoptosis (Fig. 3*B* and *SI Appendix*, Fig. S9*B*). Similar results were obtained when PIM2 was inhibited with AZD1208 (Fig. 3 *C* and *D* and *SI Appendix*, Fig. S9*C*) or a second, unrelated PIM inhibitor, LGH447 (*SI Appendix*, Fig. S9 *D* and *E*), or when *PIM2* expression was reduced following knockdown of STAT4 (*SI Appendix*, Fig. S9*F*). Notably, combined treatment with IM and AZD1208 had synergistic effects on cell viability and apoptosis (Fig. 3 *C* and *D*). In addition, combined treatment with IM and AZD1208 synergistically suppressed colony formation of human primary $CD34^+$ CML cells (Fig. 3*E* and *SI Appendix*, Fig. S9*G*). Combined IM and AZD1208 treatment also significantly reduced the viability of two wild-type BCR-ABL IM-resistant CML cell lines, KCL22 (*SI Appendix*, Fig. S9*H*) and K562R (31) (*SI Appendix*, Fig. S9 *I* and *J*), and CML cells from IM-resistant patients harboring wild-type BCR-ABL (*SI Appendix*, Fig. S9*K*). Of note, however, the combined drug treatment had a negligible effect on the viability of HSCs (Fig. 3*F*).

In contrast to *PIM2*, our single-cell RNA-seq analysis did not identify *PIM1* or *PIM3* as significantly up-regulated in CMLSCs (Dataset S1). We confirmed that of the three PIM family members, PIM2 plays a major role in contributing to the IM resistance of CMLSCs and KCL22 cells and is the critical target of AZD1208 (*SI Appendix*, Fig. S10).

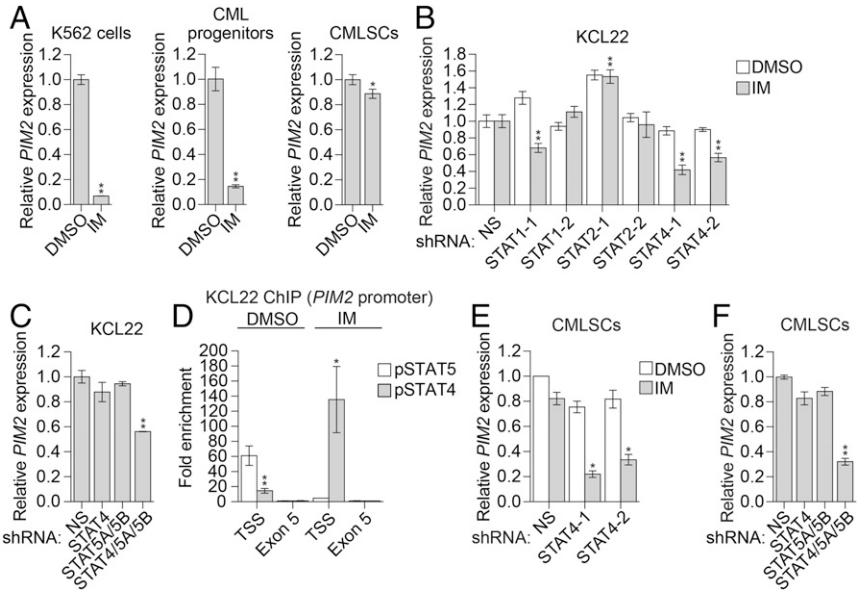

Fig. 2. *PIM2* expression in CMLSCs is promoted by both a BCR-ABL–dependent STAT5-mediated pathway and a BCR-ABL–independent STAT4-mediated pathway. (*A*) qRT-PCR monitoring of *PIM2* expression following IM treatment in K562 cells, CML progenitors ($CD34^+CD38^+$), and CMLSCs ($CD34^+CD38^-CD90^+$). Error bars indicate SD. $n = 3$ technical replicates of a representative experiment (out of two independent experiments). (*B*) qRT-PCR monitoring of *PIM2* expression in KCL22 cells expressing a nonsilencing (NS) shRNA or one of two unrelated STAT1, STAT2, or STAT4 shRNAs and treated in the presence or absence of 1 μM IM. Error bars indicate SD. $n = 3$ technical replicates of a representative experiment (out of at least two experiments). (*C*) qRT-PCR monitoring of *PIM2* expression in KCL22 cells expressing an NS, STAT4, and/or STAT5A/STAT5B shRNAs. Error bars indicate SD. $n = 3$ technical replicates of a representative experiment (out of at least two experiments). (*D*) ChIP analysis monitoring enrichment of phosphorylated STAT4 (pSTAT4) and phosphorylated STAT5 (pSTAT5) on the *PIM2* promoter at the transcription start site (TSS) or, as a control, exon 5 in the presence or absence of IM. The results were normalized to those obtained at exon 5, which was set to 1. Error bars indicate SEM. $n = 2$ biological replicates. (*E*) qRT-PCR monitoring of *PIM2* levels in CMLSCs ($CD34^+CD38^-CD90^+$) expressing an NS or STAT4 shRNA and treated in the presence or absence of IM. Error bars indicate SD. $n = 4$ technical replicates of a single experiment. (*F*) qRT-PCR monitoring of *PIM2* expression in CMLSCs ($CD34^+CD38^-CD90^+$) expressing an NS, STAT4, and/or STAT5A/STAT5B shRNAs. Error bars indicate SD. $n = 3$ technical replicates of a representative experiment (out of two experiments). $^*P \leq 0.05$; $^{**}P \leq 0.01$.

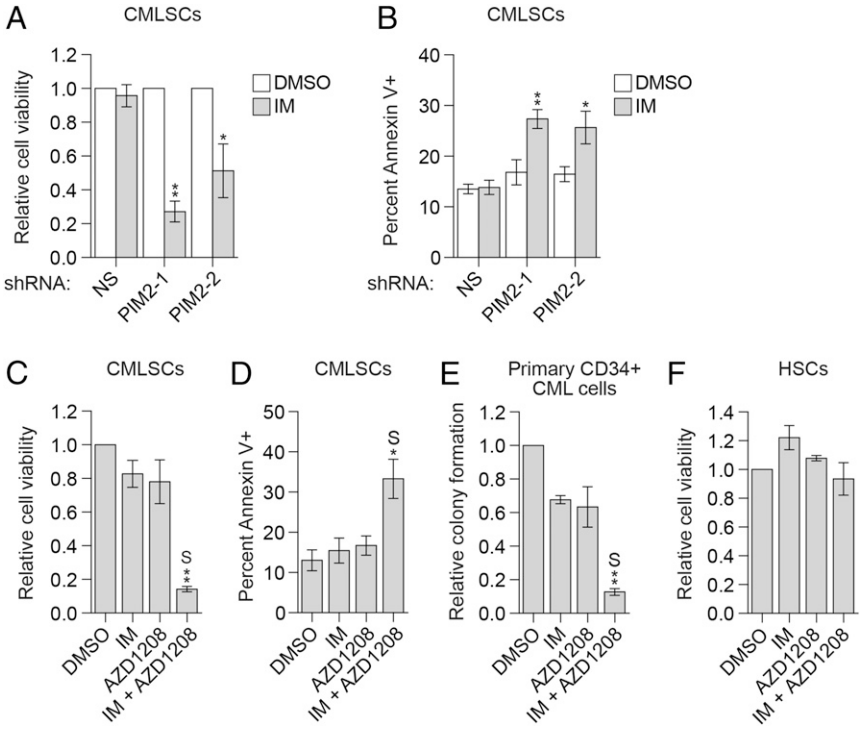

Fig. 3. Combined treatment with IM and the PIM inhibitor AZD1208 synergistically increases the apoptosis of CMLSCs and suppresses colony formation. (*A* and *B*) Relative cell viability (*A*) and apoptosis (*B*) of CMLSCs ($CD34^+CD38^-CD90^+$) from CML patient samples expressing an NS or *PIM2* shRNA and treated with DMSO or IM. In *A*, the results were normalized to those obtained in DMSO-treated cells, which was set to 1. Error bars indicate SEM. $n = 4$ biological replicates. (*C* and *D*) Relative cell viability (*C*) and apoptosis (*D*) of CMLSCs ($CD34^+CD38^-CD90^+$) from CML patient samples treated with DMSO, IM, AZD1208, or both IM and AZD1208. Error bars indicate SEM. $n = 4$ biological replicates. (*E*) Colony-formation assay of human primary $CD34^+$ CML cells treated with DMSO, IM, AZD1208, or both IM and AZD1208. To perform synergy analysis, the data from four individual CML patients (shown in *SI Appendix*, Fig. S9*G*) were combined and normalized by setting DMSO treatment to 1. Error bars indicate SEM. $n = 4$ biological replicates. (*F*) Relative cell viability of normal HSCs from healthy donors treated with DMSO, IM, AZD1208, or both IM and AZD1208. Error bars indicate SEM. $n = 3$ biological replicates. S denotes the combined drug treatment was synergistic. $^*P \leq 0.05$; $^{**}P \leq 0.01$.

Combined Treatment with IM and the PIM Inhibitor AZD1208 Significantly Prolongs Survival in a Mouse CML Model. We next asked whether combined IM and AZD1208 treatment could eradicate CMLSCs in a conventional mouse model of CML (*SI Appendix*, Fig. S11*A*). We found that combined treatment with IM and AZD1208 significantly delayed the relapse of CML disease (Fig. 4*A*), synergistically increased apoptosis in the CML LSK population (Fig. 4*B* and *SI Appendix*, Fig. S11*B*), and significantly reduced the total numbers of CML LSK cells (Fig. 4*C*), short-term HSCs, and long-term HSCs (Fig. 4*D*) but spared normal LSK cells (Fig. 4*E*). In addition, expansion of CML cells in the peripheral blood of secondary recipients was significantly slower following treatment with both drugs (*SI Appendix*, Fig. S11*C*). Most importantly, mice receiving bone marrow from donors treated with IM and AZD1208 survived significantly longer (Fig. 4*F*), indicative of a reduced number of transplantable CMLSCs. Combined IM and AZD1208 treatment also synergistically reduced the number of CMLSCs in a CML patient-derived xenograft mouse model (*SI Appendix*, Fig. S11*E*).

Discussion

Prosurvival genes that are preferentially expressed in CMLSCs compared with normal HSCs represent potential therapeutic targets for selectively eradicating IM-resistant CMLSCs. In this study, we identified *PIM2* as one of the most highly and significantly up-regulated genes in CMLSCs, and went on to characterize its role in promoting IM resistance in CMLSCs. We note that a previous single-cell RNA-seq study did not identify *PIM2* as a differentially expressed gene between HSCs versus CMLSCs (32), perhaps because they analyzed the less-enriched $CD34^+CD38^-$ population rather than the more primitive $CD34^+CD38^-CD90^+CD45RA^-$ cells, used here.

Our major conclusions are summarized in the model of Fig. 5 and discussed below. In IM-sensitive CML cells, BCR-ABL promotes *PIM2* expression through STAT5 and also initiates several other survival pathways (33). Inhibition of BCR-ABL by IM results in reduced levels of *PIM2* and decreased levels of pBAD, as well as inhibition of other survival pathways, leading to cell death. In IM-resistant CMLSCs, *PIM2* expression is promoted by both a BCR-ABL–dependent (IM-sensitive) STAT5-mediated pathway and a BCR-ABL–independent (IM-resistant) STAT4-mediated pathway. Thus, IM treatment alone does not lead to a reduction in PIM2 levels or loss of pBAD, and cell survival is maintained by antiapoptotic BCL-2 family members. Our model is consistent with previous studies showing that a pan-BCL-2 inhibitor can sensitize CMLSCs to IM, demonstrating a role for the BCL-2 prosurvival pathway in IM resistance (34, 35).

Most importantly, the IM resistance mechanism that we describe is therapeutically targetable, which we demonstrate by showing that combined treatment with IM and a PIM inhibitor synergistically kills CMLSCs in cell culture, eradicates human CMLSCs in a CML patient-derived xenograft mouse model, and significantly prolongs survival in a conventional mouse CML model, with a negligible effect on HSCs. Interestingly, it has been reported that the pan-PIM inhibitor SGI-1776 enhances the ability of IM to induce apoptosis in IM-sensitive CML cells (36). Of note, however, this study did not investigate the effects of SGI-1776 on IM-resistant CMLSCs.

In principle, prosurvival genes that are preferentially expressed in cancer cells can be identified by comparing the gene expression profiles of normal and cancer cells. However, this strategy is often impeded by the inability to completely separate normal and cancer cells and by the confounding effects of individual variation in gene expression profiles. Here, using CML as a model system, we describe a strategy by which HSCs and CMLSCs can be distinguished based on the presence or absence of a characteristic genetic marker, BCR-ABL. Moreover, by comparing single-cell RNA-seq results of HSCs and CMLCs isolated from the same patient, we eliminate the potential masking effect of the often-substantial differences in gene expression among individuals (37). The experimental approach that we have described can be generally applied to other malignancies that harbor oncogenic fusion proteins or other characteristic genetic markers.

Materials and Methods

CML Patient Samples. Frozen samples isolated from patients with chronic-phase CML (*SI Appendix*, Table S1) were obtained from the UMass Cancer

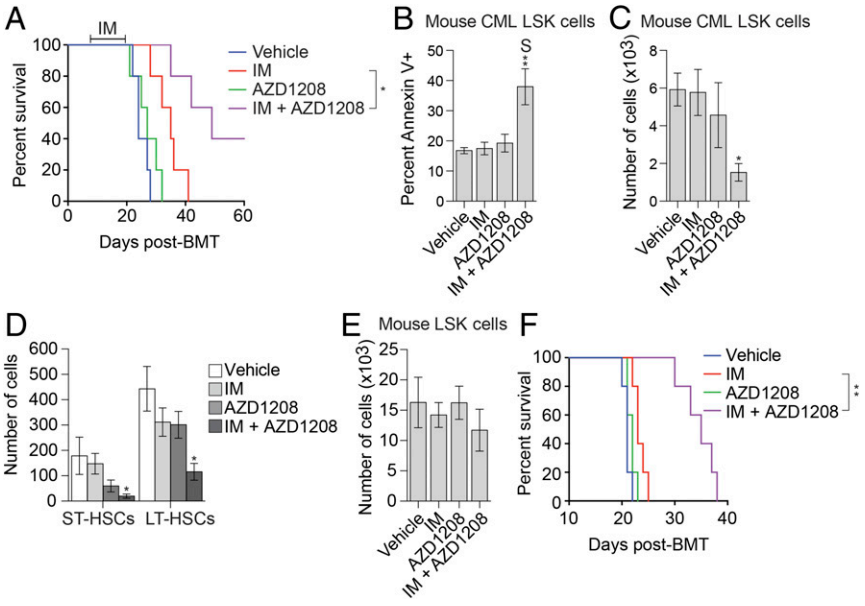

Fig. 4. Combined treatment with IM and the PIM inhibitor AZD1208 significantly prolongs survival in a mouse CML model. (*A*) Kaplan–Meier survival curve of CML mice ($n = 5$ per group) treated for 2 wk (days +7–+21) with vehicle, IM, AZD1208, or both IM and AZD1208. (*B*) Annexin-V staining monitoring apoptosis of CML LSK cells from CML mice treated with vehicle ($n = 10$), IM ($n = 9$), AZD1208 ($n = 10$) or both IM and AZD1208 ($n = 9$). (*C*–*E*) FACS determination of the number of CML (GFP^+) LSK cells (*C*), CML (GFP^+) short-term HSCs (ST-HSCs) and long-term HSCs (LT-HSCs) (*D*), or normal (GFP^-) LSK cells (*E*) after treatment of mice with vehicle ($n = 6$), IM ($n = 6$), AZD1208 ($n = 6$), or both IM and AZD1208 ($n = 5$). (*F*) Kaplan–Meier survival curve showing CML engraftment and progression in secondary transplanted mice ($n = 5$) with bone marrow cells from each group of the primary transplanted CML mice shown in *A*. S denotes the combined drug treatment was synergistic. $^*P \leq 0.05$; $^{**}P \leq 0.01$.

Center Tissue and Tumor Bank and Department of Pathology, UMass Medical School and the Druker Laboratory at Oregon Health and Science University's Knight Cancer Institute, which procured samples with approval from the Institutional Review Board (IRB #4422). Human CML samples were selected on the basis of sample availability and the requirement to achieve statistical significance. Samples were thawed at 37 °C. To avoid clumping during centrifugation, cells were immediately transferred to 20 mL of IMDM medium (STEMCELL Technologies) containing 20% FBS (Atlanta Biologicals) and 0.1 mg/mL DNaseI (Sigma-Aldrich) and incubated in a 37 °C water bath for 15–20 min. Cells were then pelleted at 300 × *g* for 10 min and either stained for HSC isolation or subjected to cell culture (*SI Appendix, Materials and Methods*).

Single-Cell RNA-Seq. Experimental details for single-cell sorting and cDNA synthesis, nested qRT-PCR to identify BCR-ABL transcripts in single cells, and single-cell RNA-seq data analysis are provided in *SI Appendix, Materials and Methods*. The RNA-seq data have been deposited in the National Center for Biotechnology Information's Gene Expression Omnibus (accession no. GSE81730).

CML Mice. All animal protocols were approved by the Institutional Animal Care and Use Committee at UMass Medical School (A-2300). Animal sample sizes were selected based on precedent established from previous publications and an understanding that at least $n = 5$ is generally required to achieve statistical significance. Mice were randomly allocated to each group for drug treatment after bone marrow transplantation and were subsequently analyzed in a nonblinded fashion. Animals were excluded from the study based on preestablished criteria: death within 10 d, with no evidence of enlarged spleen, indicative of bone marrow engraftment failure. Based on these criteria, one mouse in the IM+AZD1208-treated group was excluded (Fig. 4 *C*–*E*).

CML was induced in 6- to 8-wk old male C57BL/6 mice (The Jackson Laboratory) using retrovirus transduction as described previously (29, 38). At day +7 after bone marrow transplantation, mice were randomly grouped ($n = 5$ per group) and treated with vehicle [0.5% hydroxypropylmethycellulose (viscosity 40–60 cP, H8384, Sigma-Aldrich) and 0.2% Tween-80 in filtered ddH_2O], IM (100 mg/kg), AZD1208 (30 mg/kg), or a combination of IM and AZD1208 for approximately 2 wk, until the first vehicle-treated mouse died. Mice were monitored for survival.

For apoptosis and stem cell viability analysis, CML mice ($n = 6$ per group) were treated for 2 wk and then killed to harvest bone marrow cells for analysis as described previously (29). BCR-ABL$^+$ (GFP^+) and BCR-ABL$^-$ (GFP^-) mouse stem cells (LSK cells) were isolated from the mice by FACS as described previously (29). For secondary transplantation, all the bone marrow cells from the same group of mice were combined, and the percentage of GFP^+ cells was determined by FACS analysis. An equal number of total bone

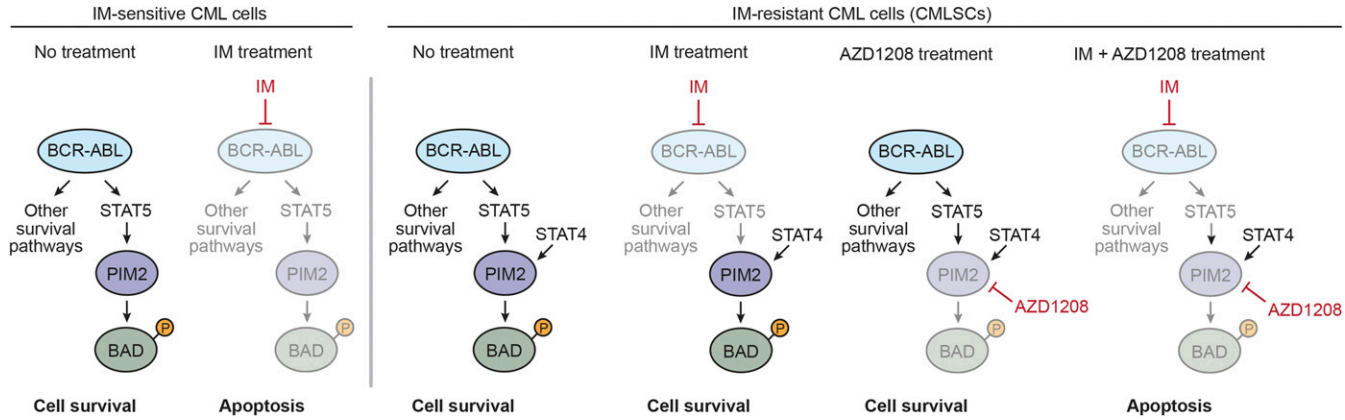

Fig. 5. Model for *PIM2* regulation in IM-sensitive and IM-resistant CML cells. In IM-sensitive CML cells, BCR-ABL promotes *PIM2* expression through STAT5 and also initiates several other survival pathways. Inhibition of BCR-ABL by IM results in reduced levels of *PIM2*, inhibition of other survival pathways, and cell death. In IM-resistant CMLSCs, *PIM2* expression is promoted by both a BCR-ABL–dependent (IM-sensitive) STAT5-mediated pathway and a BCR-ABL–independent (IM-resistant) STAT4-mediated pathway. Thus, IM treatment alone does not lead to a reduction in PIM2 levels, and cell survival is maintained. Combined treatment with IM and a PIM inhibitor (AZD1208) results in reduced levels of *PIM2* and cell death.

marrow cells were transplanted into lethally irradiated secondary recipients. Mice were monitored for accumulation of CML cells (GFP^+ cells) in peripheral blood and survival.

Pim2 expression was analyzed in mouse LSK cells and LT-HSCs (*SI Appendix*, Figs. S5 *C* and *D* and S7*G*) using Tet-off SCL-tTA/BCR-ABL transgenic mice, bred as described previously (39). To induce CML, BCR-ABL transgenic mice were subjected to tetracycline-water withdrawal starting at age 8 wk, and CML development was monitored by FACS analysis of peripheral $Gr1^+$/$Mac1^+$ cells, which typically reached 20–30% after 2 wk of induction. Mice were treated with vehicle or IM (100 mg/kg) for another 2 wk and then killed, after which bone marrow was collected for FACS sorting of LSK cells and LT-HSCs. Mice of the same age but maintained with tetracycline-water since birth served as the normal control group. Ultra-low cell number qRT-PCR was used to determine *Pim2* expression using the primers listed in *SI Appendix*, Table S2.

Statistical Analysis. To achieve statistical significance, all qRT-PCR data were collected from experiments performed in technical triplicate. Each experiment was repeated at least twice, and statistically significant results were obtained in independent biological replicates. Differences between groups were assayed with the two-tailed Student *t* test using GraphPad Prism. In cases where the assumption of the *t* test was not valid, a nonparametric statistical method (e.g., Mann–Whitney *U* test) was used. Significant differences were considered when $P < 0.05$. Data are presented as mean ± SD or SEM, as indicated in the figure legends.

Statistical analysis for drug synergy was performed using R version 3.5.0, a system for statistical computation and graphics (40), to assess whether the combined effects from IM and AZD1208/LGH447 were synergistic (greater than the sum of the single-drug effects) or nonsynergistic. The number of surviving cells or percentages were rank-transformed, followed by two-way ANOVA to test the main effect and the interaction of the two drugs with a randomized complete block design (Fig. 3 *C*, *E*, and *F*) or a completely randomized design (Fig. 4 *C*–*E* and *G*). The percentage of viable cells was transformed using the logit function, followed by two-way ANOVA with a randomized complete block design (Fig. 3*D*) or a completely randomized design (Fig. 4*B*).

To determine whether IM and AZD1208/LGH447 exerted synergistic impacts on decreasing cell survival, we compared the difference between observed effects with the expected additive effects for the mouse/patient samples exposed to both drugs (41). The difference was estimated as the interaction coefficient in the ANOVA. If there was a significant negative difference (i.e., interaction coefficient <0 and $P < 0.05$), then the impact from the combined drugs was classified as synergistic; otherwise, it was classified as nonsynergistic. For apoptosis, if there was a significant positive difference, then the impact from the combined drugs was classified as synergistic; otherwise, it was classified as nonsynergistic. When there was no statistically significant synergistic effect, combined drug treatments were compared with IM treatment alone using a predetermined contrast under the ANOVA framework.

Additional information on the materials and methods used for GSEA, ultra-low cell number qRT-PCR, CML patient sample culturing for functional experiments, phospho-flow analysis, immunoblot analysis, shRNA-mediated knockdown, data mining, ChIP, relative cell viability and apoptosis assays, ectopic PIM expression, colony-formation assays, and PDX mice experiments are available in *SI Appendix, Materials and Methods*.

ACKNOWLEDGMENTS. We thank Karl Simin and Brian Druker for providing CML samples; Nicholas Donato for providing K562R cells, Amy Virbasius and the UMass Medical School RNAi Core Facility for providing shRNAs and MGC clones; the UMass Medical School Deep Sequencing Core Facility for performing deep sequencing; and Sara Deibler for providing editorial assistance. This work was supported by National Institutes of Health Grant R01 CA163926 (to M.R.G.).

1. Faderl S, et al. (1999) The biology of chronic myeloid leukemia. *N Engl J Med* 341:164–172.
2. Deininger MW, Goldman JM, Melo JV (2000) The molecular biology of chronic myeloid leukemia. *Blood* 96:3343–3356.
3. Kurzrock R, Kantarjian HM, Druker BJ, Talpaz M (2003) Philadelphia chromosome-positive leukemias: From basic mechanisms to molecular therapeutics. *Ann Intern Med* 138:819–830.
4. Colicelli J (2010) ABL tyrosine kinases: Evolution of function, regulation, and specificity. *Sci Signal* 3:re6.
5. Steelman LS, et al. (2004) JAK/STAT, Raf/MEK/ERK, PI3K/Akt and BCR-ABL in cell cycle progression and leukemogenesis. *Leukemia* 18:189–218.
6. An X, et al. (2010) BCR-ABL tyrosine kinase inhibitors in the treatment of Philadelphia chromosome-positive chronic myeloid leukemia: A review. *Leuk Res* 34:1255–1268.
7. Graham SM, et al. (2002) Primitive, quiescent, Philadelphia-positive stem cells from patients with chronic myeloid leukemia are insensitive to STI571 in vitro. *Blood* 99:319–325.
8. Corbin AS, et al. (2011) Human chronic myeloid leukemia stem cells are insensitive to imatinib despite inhibition of BCR-ABL activity. *J Clin Invest* 121:396–409.
9. Holyoake TL, Vetrie D (2017) The chronic myeloid leukemia stem cell: Stemming the tide of persistence. *Blood* 129:1595–1606.
10. Hamilton A, et al. (2012) Chronic myeloid leukemia stem cells are not dependent on Bcr-Abl kinase activity for their survival. *Blood* 119:1501–1510.
11. Carter BZ, Mak DH, Cortes J, Andreeff M (2010) The elusive chronic myeloid leukemia stem cell: Does it matter and how do we eliminate it? *Semin Hematol* 47:362–370.
12. Sloma I, Jiang X, Eaves AC, Eaves CJ (2010) Insights into the stem cells of chronic myeloid leukemia. *Leukemia* 24:1823–1833.
13. Ma L, Green M (2019) Single cell gene expression profiling in normal HSCs and CML stem cells. NCBI Gene Expression Omnibus. Available at https://www.ncbi.nlm.nih.gov/geo/query/acc.cgi?acc=GSE81730. Deposited May 23, 2016.
14. Shalek AK, et al. (2014) Single-cell RNA-seq reveals dynamic paracrine control of cellular variation. *Nature* 510:363–369.
15. Zhang B, et al. (2013) Microenvironmental protection of CML stem and progenitor cells from tyrosine kinase inhibitors through N-cadherin and Wnt-β-catenin signaling. *Blood* 121:1824–1838.
16. Nawijn MC, Alendar A, Berns A (2011) For better or for worse: The role of Pim oncogenes in tumorigenesis. *Nat Rev Cancer* 11:23–34.
17. Yan B, et al. (2003) The PIM-2 kinase phosphorylates BAD on serine 112 and reverses BAD-induced cell death. *J Biol Chem* 278:45358–45367.
18. Yang E, et al. (1995) Bad, a heterodimeric partner for Bcl-XL and Bcl-2, displaces Bax and promotes cell death. *Cell* 80:285–291.
19. Keeton EK, et al. (2014) AZD1208, a potent and selective pan-Pim kinase inhibitor, demonstrates efficacy in preclinical models of acute myeloid leukemia. *Blood* 123:905–913.
20. Mikkers H, et al. (2004) Mice deficient for all PIM kinases display reduced body size and impaired responses to hematopoietic growth factors. *Mol Cell Biol* 24:6104–6115.
21. Kuroda J, et al. (2006) Bim and Bad mediate imatinib-induced killing of Bcr/Abl^+ leukemic cells, and resistance due to their loss is overcome by a BH3 mimetic. *Proc Natl Acad Sci USA* 103:14907–14912.
22. Andersson LC, Nilsson K, Gahmberg CG (1979) K562—A human erythroleukemic cell line. *Int J Cancer* 23:143–147.
23. Adam K, et al. (2015) Control of Pim2 kinase stability and expression in transformed human haematopoietic cells. *Biosci Rep* 35:e00274.
24. de Groot RP, Raaijmakers JA, Lammers JW, Jove R, Koenderman L (1999) STAT5 activation by BCR-Abl contributes to transformation of K562 leukemia cells. *Blood* 94:1108–1112.
25. Shuai K, Halpern J, ten Hoeve J, Rao X, Sawyers CL (1996) Constitutive activation of STAT5 by the BCR-ABL oncogene in chronic myelogenous leukemia. *Oncogene* 13:247–254.
26. Hantschel O, et al. (2012) BCR-ABL uncouples canonical JAK2-STAT5 signaling in chronic myeloid leukemia. *Nat Chem Biol* 8:285–293.
27. Hurtz C, et al. (2011) BCL6-mediated repression of p53 is critical for leukemia stem cell survival in chronic myeloid leukemia. *J Exp Med* 208:2163–2174.
28. Jiang X, et al. (2007) Chronic myeloid leukemia stem cells possess multiple unique features of resistance to BCR-ABL targeted therapies. *Leukemia* 21:926–935.
29. Ma L, et al. (2014) A therapeutically targetable mechanism of BCR-ABL-independent imatinib resistance in chronic myeloid leukemia. *Sci Transl Med* 6:252ra121.
30. Quentmeier H, Eberth S, Romani J, Zaborski M, Drexler HG (2011) BCR-ABL1-independent PI3Kinase activation causing imatinib resistance. *J Hematol Oncol* 4:6.
31. Donato NJ, et al. (2004) Imatinib mesylate resistance through BCR-ABL independence in chronic myelogenous leukemia. *Cancer Res* 64:672–677, and erratum (2004) 64:2306.
32. Giustacchini A, et al. (2017) Single-cell transcriptomics uncovers distinct molecular signatures of stem cells in chronic myeloid leukemia. *Nat Med* 23:692–702.
33. Cilloni D, Saglio G (2012) Molecular pathways: BCR-ABL. *Clin Cancer Res* 18:930–937.
34. Airiau K, et al. (2012) ABT-737 increases tyrosine kinase inhibitor-induced apoptosis in chronic myeloid leukemia cells through XIAP downregulation and sensitizes CD34(+) CD38(–) population to imatinib. *Exp Hematol* 40:367–378.e2.
35. Goff DJ, et al. (2013) A Pan-BCL2 inhibitor renders bone-marrow-resident human leukemia stem cells sensitive to tyrosine kinase inhibition. *Cell Stem Cell* 12:316–328.
36. Curi DA, et al. (2015) Pre-clinical evidence of PIM kinase inhibitor activity in BCR-ABL1 unmutated and mutated Philadelphia chromosome-positive (Ph^+) leukemias. *Oncotarget* 6:33206–33216.
37. Cheung VG, et al. (2003) Natural variation in human gene expression assessed in lymphoblastoid cells. *Nat Genet* 33:422–425.
38. Zhang B, et al. (2016) Heterogeneity of leukemia-initiating capacity of chronic myelogenous leukemia stem cells. *J Clin Invest* 126:975–991.
39. Koschmieder S, et al. (2005) Inducible chronic phase of myeloid leukemia with expansion of hematopoietic stem cells in a transgenic model of BCR-ABL leukemogenesis. *Blood* 105:324–334.
40. Ihaka R, Gentleman R (1996) R: A language for data analysis and graphics. *J Comput Graph Stat* 5:299–314.
41. Slinker BK (1998) The statistics of synergism. *J Mol Cell Cardiol* 30:723–731.